Journal of Thermal Analysis and Calorimetry, Vol. 78 (2004) 487–500

APPLICATION OF COUPLED TG-FTIR SYSTEM IN STUDIES OF THERMAL STABILITY OF MANGANESE(II) COMPLEXES WITH AMINO ACIDS

*M. Sikorska-Iwan** *and R. Mrozek-Łyszczek*

Faculty of Chemistry, University of Maria Curie-Skłodowska, Maria Curie-Skłodowska Sq. 2,
20-031 Lublin, Poland

Abstract

Detailed thermal analysis of manganese(II) complexes with α-amino acids were carried out. The thermal degradation is multi-stage. Dehydration of complexes is the first mass loss step. Anhydrous compounds are unstable and decompose to Mn_3O_4 in air or to MnO in inert atmosphere. The intermediate solid products were identified by TG method and TG/FTIR combined technique. Among others solid residues, the presence of $MnSO_4$, $MnBr_2$ and $Mn(CH_3COO)Cl$ was found. In the gaseous products of decomposition of organic ligand H_2O, NH_3, CO_2, CO, aromatic and non-aromatic hydrocarbons and very probably cyanoacetic acid and dimethyl sulfide occurred. Inorganic ions, i.e. Cl^-, Br^- or SO_4^{2-} remain in the solid products of decomposition or are lost as HCl, HBr or SO_2.

Keywords: α-amino acids, manganese(II) complexes, TG-FTIR coupled technique, thermal analysis

Introduction

Thermoanalytical techniques – TG, DTA, DSC – play an important role in studying the structure, stability and some properties of metal complexes. Unfortunately, these techniques do not make it possible to identify unequivocally the products of thermal decomposition. The differentiation between an endothermic loss of solvent molecules or a vaporisation or a decomposition reaction is very difficult because not all necessary data are available. The identification of gases involved in the thermal process is indispensable. In this case the TG/FTIR coupled technique is very useful to understand the thermal degradation pathway [1].

The present paper is concerning the thermal stability of manganese(II) complexes with popular α-amino acids. A part of the results was published in [2–7]. The paper is a review, but there are many unpublished results, too. Reviewing our own work, we would like to find new correlations which were not obvious at the time the work was performed but which are now easily seen. In addition, studying the previous work we will provide some critical comments on the thermal degradation pathways of complexes.

---

* Author for correspondence: E-mail: mariolas@hermes.umcs.lublin.pl

1388–6150/2004/ $ 20.00

Akadémiai Kiadó, Budapest
Kluwer Academic Publishers, Dordrecht

Experimental

The preparation methods of manganese(II) complexes with selected α-amino acids were described previously [2–7]. Table 1 presents the formulas and some properties of studied complexes. The composition of complexes were verified by elemental analysis (Perkin Elmer CHN 2400 analyser), IR spectrophotometry in the range 4000–400 cm^{-1} using the KBr pellet technique (Specord M80 spectrophotometer) and by thermogravimetry (Setaram Setsys 16/18 thermobalance). Magnetic susceptibility measurements were conducted at 20°C using Sherwood Scientific Ltd MSB-MKI magnetic susceptibility balance.

Thermal measurements were performed with a Setaram Setsys 16/18 thermobalance in dynamic air (v=1.1 dm^3 h^{-1}) or in argon atmosphere (v=0.7 dm^3 h^{-1}), at a heating rate of 10°C min^{-1}, in open ceramic crucible. The sample mass was ~10 mg. DSC curves were obtained with a Netzsch DSC 204 apparatus. The 5–10 mg samples were heated at a rate of 1 or 2°C min^{-1} in argon atmosphere using an aluminium open crucible. The gaseous products of thermal decomposition were identified using a Netzsch TG 209 apparatus coupled with a Bruker FTIR IFS66 spectrophotometer. The samples (~10 mg) were heated in flowing argon atmosphere at a heating rate of 10°C min^{-1}.

Results and discussion

Table 1 contains the formulas and some properties of studied complexes.The studies of crystal structures and physicochemical properties of obtained complexes show the polymeric chain structure. The manganese ions are connected by carboxylic groups of amino acids molecules (1 or 2 bridges) and by chloride bridges in the case of proline and alanine complexes. The carboxylic groups act as bidentate bridging ones. The water molecules coordinate as monodentate ligands and chloride anions are monodentate or bidentate bridging in proline and alanine compounds. Because the amino groups exist as $-NH_3^+$ ions (or $-NH_2^+$- in proline or hydroxyproline), the nitrogen atoms do not take part in manganese ion coordination. They participate as proton donors in 2 hydrogen bonds, at least. The oxygen atoms coming from carboxylic groups or water molecules or SO_4^{2-} ions, or chloride ions are proton acceptors in these bonds [2–7].

The effective magnetic moments is in the range of 5.21–6.01 M.B. The value is characteristic of 5 unpaired electrons in manganese(II) ions. It indicates that the studied amino acid ligands form the high-spin complexes with Mn^{2+} ions [2–7].

Thermal stability of complexes were examined by using several techniques, i.e. TG-DTA in air and inert atmosphere, DSC and TG-FTIR. The stages of thermal decomposition, the solid products of decomposition and enthalpies of reactions are given in Table 2. The shape of TG-DTA curves indicates the multi-stage thermal decomposition. Unfortunately many intermediate solid products are difficult or impossible to be identified only by mass loss. Moreover, the values of mass loss in dehydration and deamination processes are very similar. Most of the intermediate solid products are unstable and it is not the possible to separate and identify them by

Table 1 The formulas and properties of manganese(II) complexes with α-amino acids (gly – glycine NH_2CH_2COOH; ala – alanine $NH_2CH(CH_3)COOH$; thr – threonine $CH_3CH(OH)CH(NH_2)COOH$; met – methionine $CH_3S(CH_2)_2CH(NH_2)COOH$; phe – phenylalanine $C_6H_5CH_2CH(NH_2)COOH$; glu – glutamic acid $HOOC(CH_2)_2CH(NH_2)COOH$; asp – aspartic acid $HOOCCH_2CH(NH_2)COOH$; pro – proline $HOOCCHNH(CH_2)_3$; hyp – hydroxyporoline $HOOCCHNH(CH_2)_2CH(OH)$

Formula	Crystal system (space group)	Crystal parameters	Effective magnetic moment at 20°C [M.B.]
$Mn(gly)_2Cl_2$	triclinic ($P\bar{1}$)	a=4.968(2); b=6.582(2); c=7.925(3) Å α=106.17(3); β=92.86(3); γ=107.21(3)°	5.82
$Mn(gly)Cl_2(H_2O)_2$	monoclinic ($P2_1/n$)	a=6.519(2); b=15.981(3); c=7.893(2) Å β=97.18(3)°	5.70
$Mn(gly)_2Br_2(H_2O)_2$			5.66
$Mn(gly)Br_2(H_2O)_2$			5.39
$Mn(L\text{-}ala)Cl_2(H_2O)_2$	triclinic (P1)	a=7.544(2); b=10.869(3); c=11.207(3) Å α=85.55(3); β=87.02(3); γ=82.84(3)°	5.58
$Mn(L\text{-}thr)Cl_2(H_2O)$			5.43
$Mn(L\text{-}thr)SO_4(H_2O)_2$			6.01
$Mn(L\text{-}met)Cl_2(H_2O)_2$			5.92
$Mn(L\text{-}phe)Cl_2(H_2O)_{3.5}$			5.81
$Mn(L\text{-}glu)SO_4(H_2O)$			5.87
$Mn(L\text{-}asp)Cl_2(H_2O)_3$			5.21
$Mn(L\text{-}pro)Cl_2(H_2O)$	rhombic ($P2_12_12_1$)	a=7.112(2); b=19.196(2); c=13.249(3) Å	5.71
$Mn(L\text{-}hyp)SO_4(H_2O)_4$	triclinic (P1)	a=7.478(1); b=9.297(2); c=9.814(2) Å α=87.38(3); β=67.81(3); γ=64.21(3)°	5.51

Table 2 Thermal analysis data of the compounds

Complex	Air atmosphere			
	T_{range}/°C	Mass loss/%		Residue
		found	calc.	
$Mn(gly)_2Cl_2$	150–220	5.04		
	220–285	34.75		
	285–415	54.73		
	415–700	71.43	71.38	Mn_2O_3
	850–930	72.13	72.34	Mn_3O_4
$Mn(gly)Cl_2(H_2O)_2$	85–180	15.00	15.19	$Mn(gly)Cl_2$
	185–315	37.99	36.92	$Mn(CH_3COO)Cl$
	315–420	55.46		
	420–700	66.86	66.67	Mn_2O_3
	840–930	67.84	67.79	Mn_3O_4
$Mn(gly)Br_2(H_2O)_2$	115–225	10.50	11.04	$Mn(gly)Br_2$
	235–335	27.50		
	335–550	76.50	75.75	Mn_2O_3
$Mn(gly)_2Br_2(H_2O)_2$	95–135	8.20	8.96	$Mn(gly)_2Br_2$
	210–335	32.20		
	335–620	81.00	80.30	Mn_2O_3
$Mn(L\text{-}ala)Cl_2(H_2O)_2$	70–180	14.50	14.34	$Mn(L\text{-}ala)Cl_2$
	190–290	32.37		
	290–330	43.15	42.80	Mn(L-ala)
	330–475	68.47	68.52	Mn_2O_3
$Mn(L\text{-}thr)Cl_2(H_2O)$	125–165	7.00	6.84	$Mn(L\text{-}thr)Cl_2$
	165–235	25.00		
	235–390	39.23		
	390–450	51.67		
	450–510	70.16	69.96	Mn_2O_3
$Mn(L\text{-}thr)SO_4(H_2O)_2$	75–155	11.00	11.76	$Mn(L\text{-}thr)SO_4$
	160–335	42.00		
	335–575	51.20	50.67	$MnSO_4$
	770–980	75.20	75.05	Mn_3O_4
$Mn(L\text{-}met)Cl_2(H_2O)_2$	30–150	12.60	11.57	$Mn(L\text{-}met)Cl_2$
	170–285	33.16		
	310–375	45.09		
	395–580	71.05		
	590–710	74.69	74.61	Mn_2O_3
$Mn(L\text{-}phe)Cl_2(H_2O)_{3.5}$	40–70	4.92	5.08	$Mn(L\text{-}phe)Cl_2(H_2O)_{2.5}$
	70–100	17.02	17.78	$Mn(L\text{-}phe)Cl_2$
	115–140	28.72		
	140–175	35.59		
	175–395	57.28		
	395–480	77.68	77.69	Mn_2O_3
	700–940	78.88	78.45	Mn_3O_4

Table 2 Continued

Complex	Air atmosphere			
	T_{range}/°C	Mass loss/%		Residue
		found	calc.	
$Mn(L\text{-}glu)SO_4(H_2O)$	70–90	6.00	5.70	$Mn(L\text{-}glu)SO_4$
	180–540	50.00	52.22	$MnSO_4$
	790–940	76.12	75.84	Mn_3O_4
$Mn(L\text{-}asp)Cl_2(H_2O)_3$	60–175	16.00	16.56	$Mn(L\text{-}asp)Cl_2$
	175–280	34.00		
	280–345	43.00		
	345–640	78.00		Mn_2O_3
	900–960	79.00		Mn_3O_4
$Mn(L\text{-}pro)Cl_2(H_2O)$	40–95	6.85	6.95	$Mn(L\text{-}pro)Cl_2$
	200–330	22.80		
	330–420	37.26		
	420–670	69.80		Mn_2O_3
	670–900	70.32	70.53	Mn_3O_4
$Mn(L\text{-}hyp)SO_4(H_2O)_4$	70–110	12.31	12.71	$Mn(L\text{-}hyp)(H_2O)_{1.5}SO_4$
	110–230	20.61	20.34	$Mn(L\text{-}hyp)SO_4$
	240–440	36.61		
	440–500	59.67	57.36	$MnSO_4$
	650–780	77.67	77.70	Mn_2O_3
	900–920	78.32	78.46	Mn_3O_4

Complex	Inert gas atmosphere				
	T_{range}/°C	Mass loss/%		Residue	Enthalpy/ kJ mol^{-1}
		found	calc.		
$Mn(gly)_2Cl_2$	150–280	33.20			
	280–800	75.84	74.30	MnO	
$Mn(gly)Cl_2(H_2O)_2$	85–195	15.21	15.19	$Mn(gly)Cl_2$	36.6
	200–360	39.01	36.92	$Mn(CH_3COO)Cl$	
	360–615	63.62	63.30	MnO_2	
	615–800	70.12	70.04	MnO	
$Mn(gly)Br_2(H_2O)_2$	100–200	12.15	11.04	$Mn(gly)Br_2$	86.42
	260–350	29.65			
	360–600	77.00	78.22	MnO	
$Mn(gly)_2Br_2(H_2O)_2$	110–145	7.43	8.96	$Mn(gly)_2Br_2$	92.2
	230–365	32.19			–16.5
	365–390	45.41	46.38	$MnBr_2$	
	400–640	83.05	82.29	MnO	
$Mn(L\text{-}ala)Cl_2(H_2O)_2$	70–180	14.52	14.34	$Mn(L\text{-}ala)Cl_2$	32.8+0.8
	190–260	37.79			
	260–300	43.95	42.80	Mn(L-ala)	
	300–640	66.17	65.20	MnO_2	
	640–920	71.47	71.71	MnO	

Table 2 Continued

Complex	Inert gas atmosphere				
	T_{range}/°C	Mass loss/%		Residue	Enthalpy/ kJ mol^{-1}
		found	calc.		
$Mn(L\text{-}thr)Cl_2(H_2O)$	125–165	6.90	6.84	$Mn(L\text{-}thr)Cl_2$	49.5
	165–245	25.74			
	245–440	45.89			
	440–640	65.20	66.92	MnO_2	
	640–915	73.02	73.02	MnO	
$Mn(L\text{-}thr)SO_4(H_2O)_2$	60–200	12.00	11.67	$Mn(L\text{-}thr)SO_4$	
	200–330	35.00			
	330–490	43.00			
	500–630	56.50	50.67	$MnSO_4$	
	630–710	74.00	76.80	MnO	
$Mn(L\text{-}met)Cl_2(H_2O)_2$	30–130	12.67	11.57	$Mn(L\text{-}met)Cl_2$	
	170–310	42.67			
	310–615	64.02			
	615–980	77.31	77.18	MnO	
$Mn(L\text{-}phe)Cl_2(H_2O)_{3.5}$	30–65	5.29	5.08	$Mn(L\text{-}phe)Cl_2(H_2O)_{2.5}$	
	70–100	17.62	17.78	$Mn(L\text{-}phe)Cl_2$	158.6
	110–175	21.60			
	175–250	27.58			
	250–420	60.26			
	420–985	79.20	79.95	MnO	
$Mn(L\text{-}glu)SO_4(H_2O)$	70–100	5.90	5.70	$Mn(L\text{-}glu)SO_4$	60.0
	190–240	21.00			
	240–320	31.00			
	320–520	44.50			
	520–610	76.50	77.54	MnO	
$Mn(L\text{-}asp)Cl_2(H_2O)_3$	45–65	5.77	5.52	$Mn(L\text{-}asp)Cl_2(H_2O)_2$	
	85–140	11.32	11.04	$Mn(L\text{-}asp)Cl_2(H_2O)$	45.9
	140–180	16.96	16.52	$Mn(L\text{-}asp)Cl_2$	44.1
	180–255	29.00			
	255–385	47.00			
$Mn(L\text{-}pro)Cl_2(H_2O)$	40–95	6.73	6.95	$Mn(L\text{-}pro)Cl_2$	47.6
	200–330	32.73			
	330–420	47.84			
	420–670	67.28	66.41	MnO_2	
	670–900	72.09	72.60	MnO	
$Mn(L\text{-}hyp)SO_4(H_2O)_4$	70–110	12.30	12.71	$Mn(L\text{-}hyp)(H_2O)_{1.5}SO_4$	43.5
	110–230	20.60	20.34	$Mn(L\text{-}hyp)SO_4$	53.1
	240–340	36.15			
	340–360	41.10			
	360–480	52.85	57.36	$(MnSO_4)$	
	480–600	79.72	79.94	MnO	

elemental analysis, for example. We decided to use the coupled TG-FTIR technique to resolve this problem.

Table 3 presents the gaseous products of decomposition and temperature ranges of their formation. The respective gaseous products were identified on the ground of characteristic bands: H_2O – 3500–3900, 1750–1250 cm^{-1} [8]; NH_3 – 3320, 960, 920 cm^{-1} [9, 10]; CO_2 – 3730, 3600 cm^{-1} (overtones) [11], 2360, 2330 cm^{-1} [12], 668 cm^{-1} [13]; HCl – 3100–2600 cm^{-1} [14]; HBr – 2800–2400 cm^{-1} [15]; HCN – 2280 cm^{-1} [16]; CO – 2180, 2100 cm^{-1} [9]; SO_2 – 1377, 1159, 1122 cm^{-1} [9, 15]; COS – 2080, 2050 cm^{-1} [15]; $(CH_3)_2S$ – 3000–2900, 1438, 1328, 1040 cm^{-1} [17]; non-aromatic hydrocarbons – 2975, 2900, 1450 cm^{-1} [8, 9, 11]; aromatic ring – 3100, 3050, 2970, 2940, 1400, 1000, 750 cm^{-1} [13, 14]; aldehydes – 2770–2700 cm^{-1} [18]; carbonyl group – 1770 cm^{-1} [12].

The results obtained by TG-DTA and TG-FTIR methods are in good agreement. Individual stages of thermal decomposition are observed in the same temperature ranges. Little differences (±10°C) are caused by some differences in experimental conditions, for example by different types of thermobalances. In accordance with our expectations the first stage of decomposition is connected with the loss of crystallization water molecules. The bands corresponding to NH_3 molecules appear above 250°C, except glycine complex: $Mn(gly)_2Cl_2$ when the ammonium secretion is observed at 150°C. The methionine complex $Mn(L\text{-}met)Cl_2(H_2O)_2$ represents the other exception. Up to 450°C, there are neither ammonium molecules nor other nitrogen compounds in the gaseous products of thermal decomposition (Fig. 1). Probably the nitrogen remains in solid decomposition products and it is lost above 450°C.

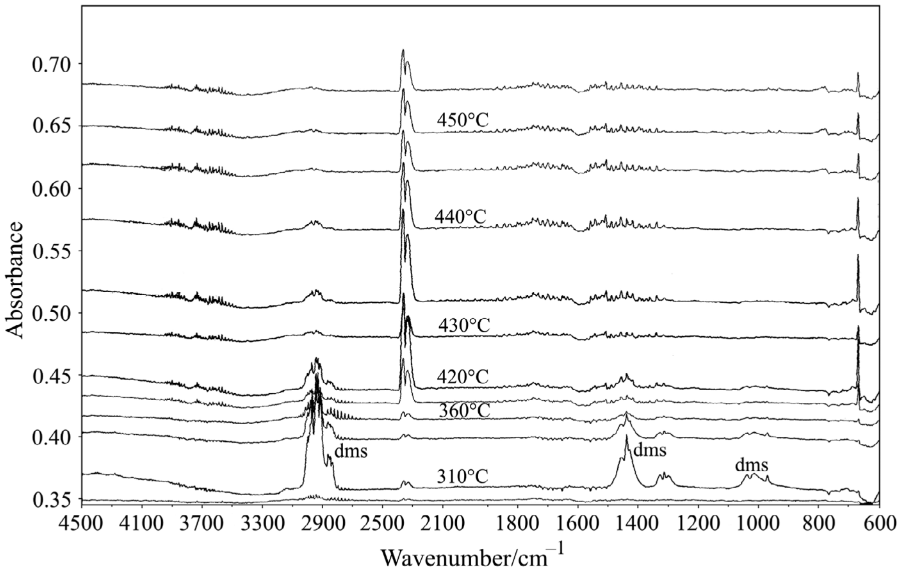

Fig. 1 FTIR spectra of gaseous products of thermal decomposition of $Mn(L\text{-}met)Cl_2(H_2O)_2$ (dms – dimethyl sulfide)

Table 3 Temperature ranges of formation of gaseous products of thermal decomposition of manganese complexes with α-amino acids (–CHO – aldehyde group; –C=O – carbonyl group; –CH– – non-aromatic hydrocarbons; $–C_6H_5$ – aromatic ring; dms – dimethyl sulphide; in the parenthesis the temperature of the most intense secretion is given) (**1** – $Mn(gly)_2Cl_2$, **2** – $Mn(gly)Cl_2(H_2O)_2$, **3** – $Mn(gly)Br_2(H_2O)_2$)

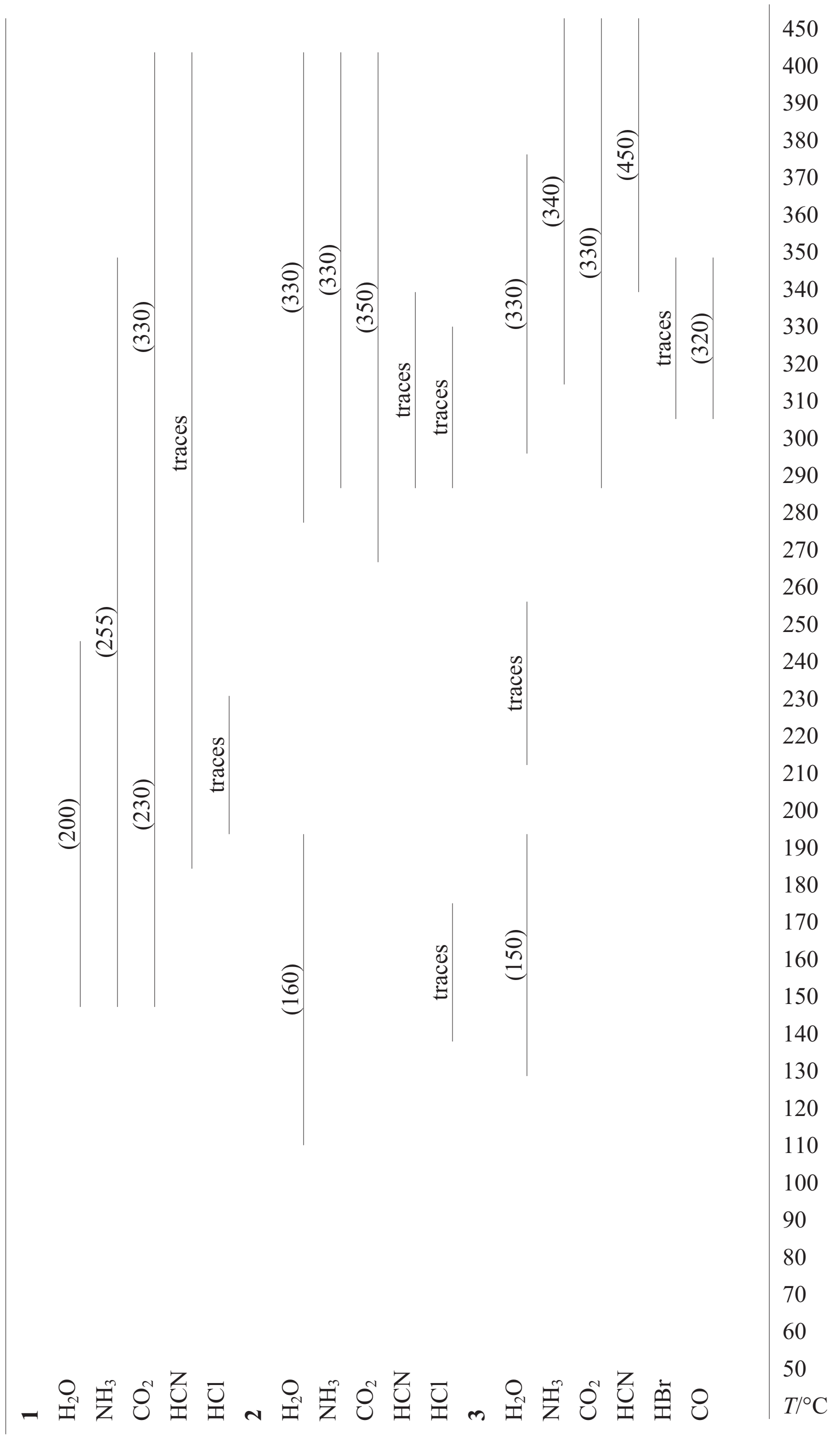

Table 3 Continued (**4** – $Mn(gly)Br_2(H_2O)_2$, **5** – $Mn(ala)Cl_2(H_2O)_2$, **6** – $Mn(thr)Cl_2(H_2O)_2$, **7** – $Mn(thr)SO_4(H_2O)_2$)

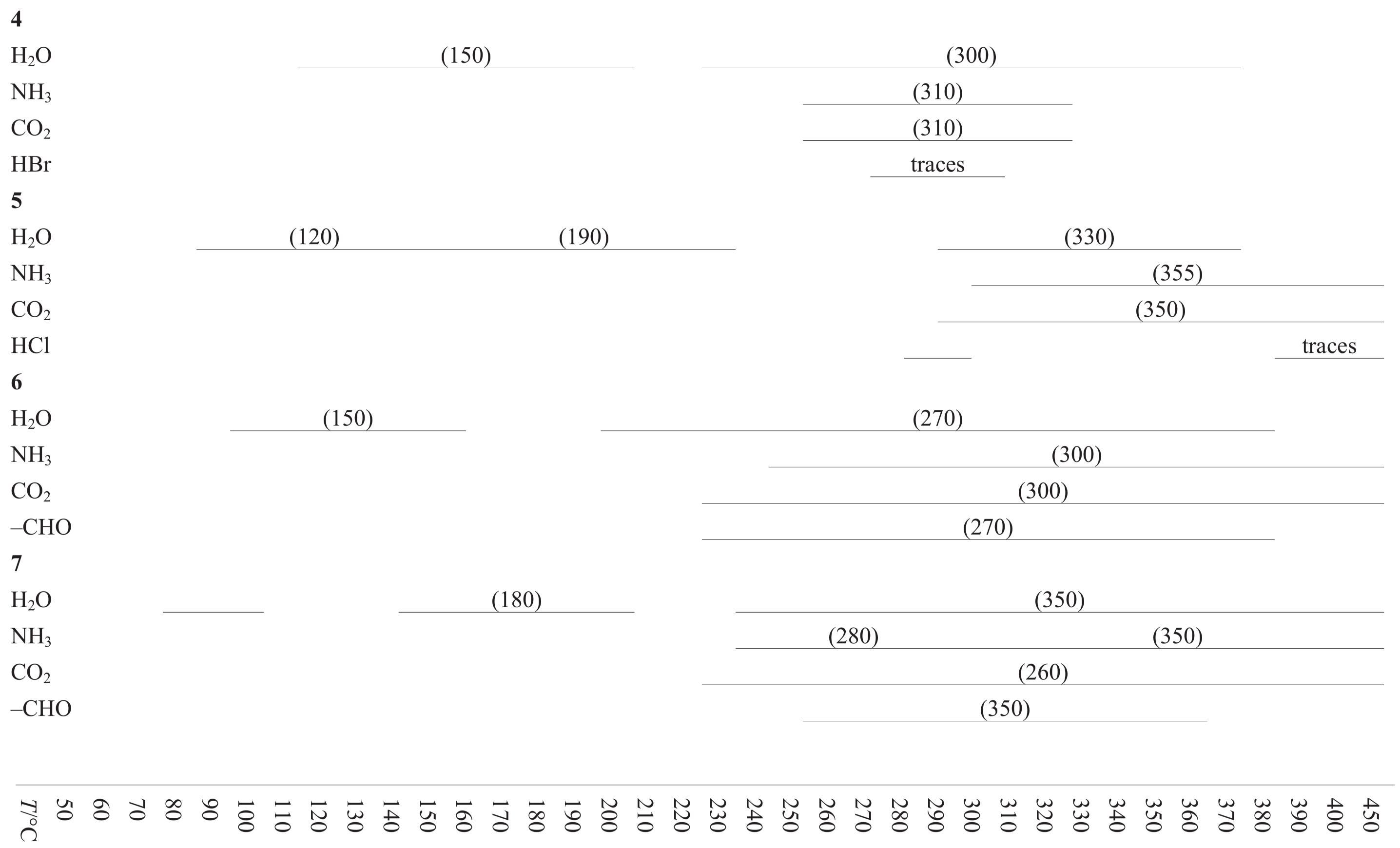

Table 3 Continued (**8** – Mn(met)$Cl_2(H_2O)_2$, **9** – Mn(phe)$Cl_2(H_2O)_{3.5}$, **10** – Mn(glu)$SO_4(H_2O)$)

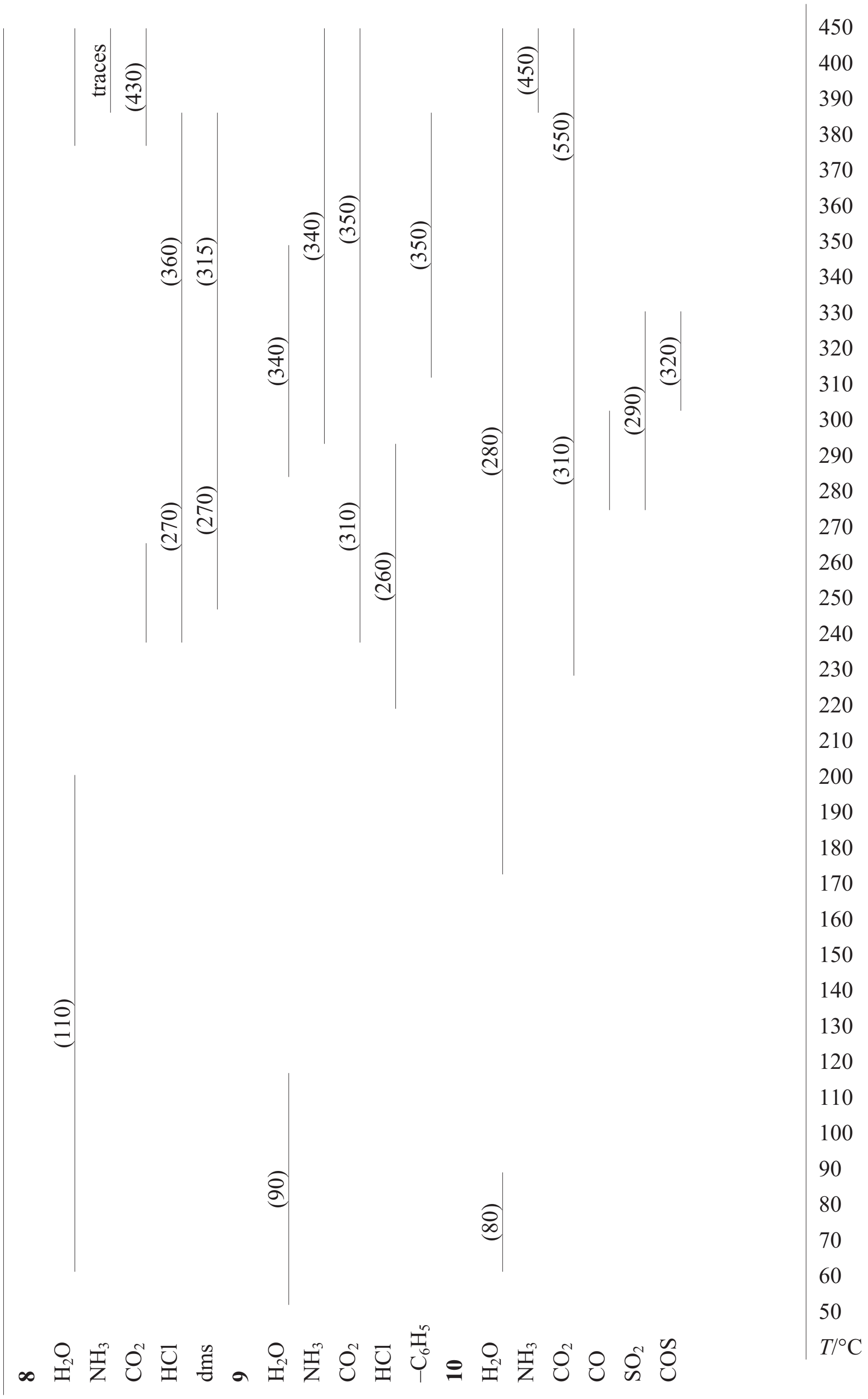

Table 3 Continued (**11** – Mn(asp)$Cl_2(H_2O)_3$, **12** – Mn(pro)$Cl_2(H_2O)$, **13** – Mn(hyp)$SO_4(H_2O)_4$

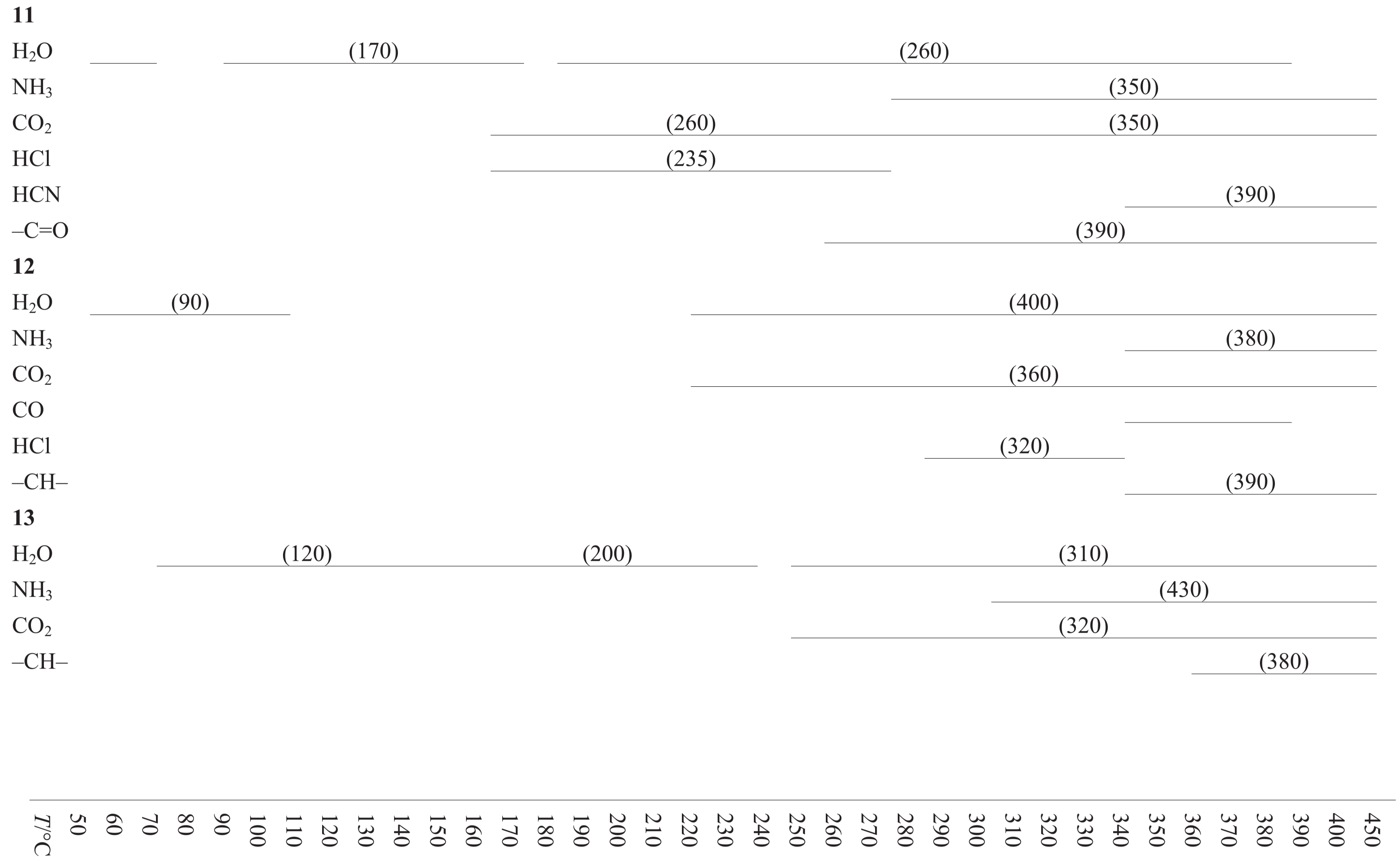

The nitrogen included in organic ligands is lost as NH_3 or HCN molecules. The complex of aspartic acid: Mn(L-asp)$Cl_2(H_2O)_3$ is particular. Its thermal decomposition is connected with the secretion of many types of gaseous products. Above 260°C a band corresponding to carbonyl group –C=O appears. A detailed analysis of FTIR spectra shows that there are two different gaseous products of decomposition containing carbonyl group: the first one appears in the range of 260–340°C, and the other one – above 340°C (Fig. 2). It is difficult to identify them. We can only suggest that the cyanoacetic acid is the second one (the characteristic bands: 3500, 2380, 2300, 1800, 1120, 680 cm^{-1} [19]).

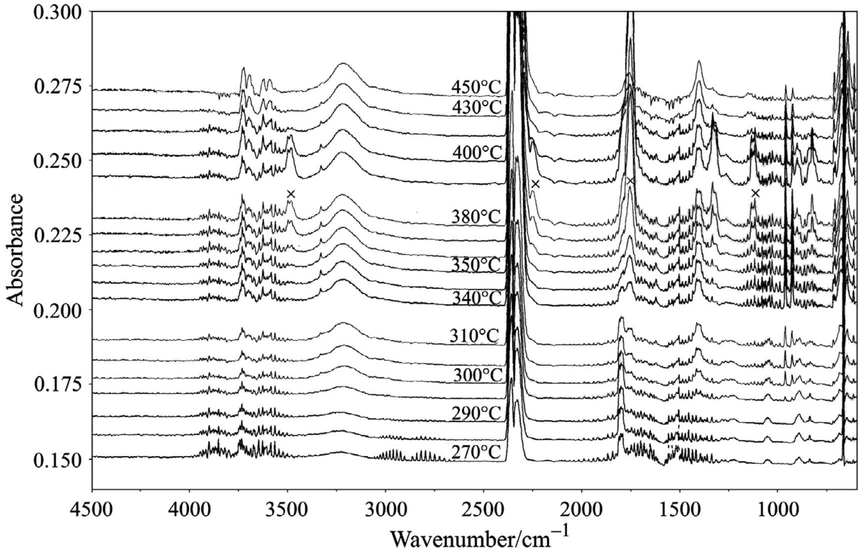

Fig. 2 FTIR spectra of gaseous products of thermal decomposition of Mn(L-asp)$Cl_2(H_2O)_3$ (*x*-cyanoacetic acid bands)

The sulfur included as SO_4^{2-} ions rests in solid decomposition products forming $MnSO_4$ (the threonine or hydroxyproline complexes) or is lost as a mixture of SO_2 and COS (the complex of glutamic acid). The decomposition of methionine molecules is more complicated. There are not SO_2 or COS bands in FTIR spectra (Fig. 1). Probably, in the range of 260–420°C dimethyl sulfide appears among the gaseous product of decomposition [17]. The supposition is confirmed by the fact that CO_2 and H_2O molecules derived from organic ligand decomposition are present in gaseous products above 400°C. The $(CH_3)_2S$ molecule formation needs the carbon and hydrogen atoms and CO_2 and H_2O appear just when dimethyl sulfide secrection is finished.

The chloride anions are released as HCl molecules. The bromide anions probably rest in solid products of decomposition. Only traces of HBr appear in spectra of gaseous products of decomposition of Mn(gly)$Br_2(H_2O)_2$ and Mn(gly)$_2Br_2(H_2O)_2$. In the case of decomposition of Mn(gly)$_2Br_2(H_2O)_2$ in inert atmosphere the mass loss in 400°C corresponds to $MnBr_2$ as solid intermediate product.

In the course of thermal decomposition of phenylalanine complex the bands of aromatic ring appear in the FTIR spectra of gaseous products, and in the case of proline and hydroxyproline compounds – the non-aromatic hydrocarbons come into being.

During the thermal decomposition of $Mn(L\text{-}ala)Cl_2(H_2O)_2$ the presence of very unstable intermediate product is observed at 300°C. The lack of data makes the identification very difficult. On the basis of mass loss we propose the Mn(L-ala) formation. The FTIR gaseous spectra show the presence of HCl in the range of 280–290°C. It seems to confirm the possibility of Mn(L-ala) formation at 300°C.

The analysis of gaseous products of thermal decomposition is very useful to identify the solid ones, but it is not sufficient. The decomposition of $Mn(gly)Cl_2(H_2O)_2$ gives the solid intermediate product which can be identify by mass loss as $Mn(CH_3COO)Cl$. Unfortunately, the gas analysis is unable to confirm it.

The final product of the thermal decomposition of studied manganese complexes in inert gas atmosphere is MnO which is formed above 600°C. In several cases the MnO is preceded by MnO_2 formation. The temperature of manganese oxide formation coincides with the end of gaseous product formation.

The compounds having a very similar composition, for example $Mn(gly)Cl_2(H_2O)_2$ and $Mn(gly)Br_2(H_2O)_2$, decompose in a different way. There is no reason for suggesting that the way of thermal decomposition of manganese complexes with amino acids is associated with any type of organic or inorganic ligand.

Conclusions

The thermal decomposition of manganese(II) complexes with amino acids is multistage. The dehydration process is the first step. The decomposition of organic ligands is the next one. The manganese oxides are the final products.

Thermogravimetry does not give all necessary data for the identification of solid intermediate products of thermal decomposition. The identification of gases involved is indispensable. FTIR analysis of gaseous decomposition products shows the H_2O, NH_3, CO_2, CO, HCl, SO_2, COS, aldehydes, aromatic and non-aromatic hydrocarbons presence. The release of dimethyl sulfide and cyanoacetic acid is very probable.

The results of TG-DTA and TG-FTIR methods are in good agreement. Analysis of gaseous products of thermal decomposition gives the possibility to separate some decomposition stages which overlap on TG-DTA curves.

The way of thermal decomposition of manganese complexes with amino acids is not associated with any type of organic or inorganic ligand.

References

1 J. M. Rollinger, Cs. Novák, Zs. Éhen and K. Marthi, J. Therm. Anal. Cal., 73 (2003) 519.
2 Z. Rzączyńska, R. Mrozek and T. Głowiak, J. Chem. Crystallogr., 27 (1997) 417.
3 R. Mrozek, Z. Rzączyńska and T. Głowiak, Monatsh. Chem., 129 (1998) 129.
4 R. Mrozek, Z. Rzączyńska, M. Sikorska-Iwan and T. Głowiak, J. Chem. Crystallogr., 29 (1999) 803.

5 R. Mrozek, Z. Rzączyńska, M. Sikorska-Iwan, M. Jaroniec and T. Głowiak, Polyhedron, 18 (1999) 2321.
6 R. Mrozek, Z. Rzączyńska and M. Sikorska-Iwan, J. Therm. Anal. Cal., 63 (2001) 839.
7 Z. Rzączyńska, R. Mrozek and M. Sikorska-Iwan, Polish J. Chem., 76 (2002) 29.
8 G. Reggers, M. Ruysen, R. Carleer and J. Mullens, Thermochim. Acta, 295 (1997) 107.
9 P. Moulinié, R. M. Paroli, Z. Y. Wang, A. H. Delgado, A. L. Guen, Y. Qi and J.-P. Gao, Polymer Test., 15 (1996) 75.
10 S. Materazzi, R. Curini, G. D'Ascenzo and A. D. Magri, Thermochim. Acta, 264 (1995) 75.
11 J. Suuronen, I. Pitkänen, H. Halttunen and R. Moilanen, J. Therm. Anal. Cal., 69 (2002) 359.
12 S. Hirose, T. Hatakeyama, Y. Izuta and H. Hatakeyama, J. Therm. Anal. Cal., 70 (2002) 853.
13 M. K. Rotich, M. E. Brown and B. D. Glass, J. Therm. Anal. Cal., 73 (2003) 499.
14 W. Xie and W.-P. Pan, J. Therm. Anal. Cal., 65 (2001) 669.
15 M. W. Chase, J. Phys. Chem. Ref. Data, Monograph, 9 (1998) 1.
16 C. Devallencourt, J. M. Saiter, A. Fafet and E. Ubrich, Thermochim. Acta, 259 (1995) 143.
17 Tables of NIST/EPA Gas-Phase Infrared Database, CAS Registry No. 71-43-2.
18 P. S. Bhandare, B. K. Lee and K. Krishnan, J. Thermal Anal., 49 (1997) 361.
19 Tables of NIST/EPA Gas-Phase Infrared Database, CAS Registry No. 372-09-8.